Phys. Status Solidi A **206**, No. 1, 173–178 (2009) / **DOI** 10.1002/pssa.200723672

physica status solidi a
www.pss-a.com
applications and materials science

# General theoretical considerations on nanowire solar cell designs

**A. Kandala[1], T. Betti[1,2], and A. Fontcuberta i Morral[*,1]**

[1] Walter Schottky Institut, Technische Universität München, Am Coulombwall 3, 85748 Garching, Germany
[2] Faculty of Electrical Engineering, University of Split, Split, Croatia

Received 29 December 2007, revised 28 May 2008, accepted 6 August 2008
Published online 18 September 2008

**PACS** 84.60.Jt, 85.30.De, 85.35.–p

[*] Corresponding author: e-mail annafm@wsi.tum.de

We propose two novel solar cell designs, tapping the advantages of semiconductor nanowires. A silicon (Si) tandem cell can be achieved by growing sub-5 nm p–n junction in the radial direction of the Si nanowires on a planar crystalline Si cell. For series connected sub-cells, based on a size-band gap dependence obtained from Quantum Monte Carlo calculations, we obtained the maximum detailed balance limit of efficiency to be 48% and 37% for concentrated and unconcentrated sunlight, respectively, for a nanowire diameter of 3.6 nm. The same efficiency would be obtained if the top tandem cell would be composed of AlGaAs nanowires, with an Al content of 19%. Ultra-high efficiencies could be achieved by a radial p–n junction nanowire tandem cell, since it could enable growth of lattice mismatched sub-cells whose band gap energies can be optimized and secondly, due to decoupling of carrier collection and light absorption. However, for a parallel connection of the sub cells, we show that the detailed balance limit of efficiency for the tandem cell will always be lower than an optimized single junction. Finally, we discuss future challenges and directions in realizing the designs.



**1 Introduction** Highest efficiencies have been obtained from multi-junction semiconductor solar cells thanks to their ability to utilize a far greater portion of the solar spectrum as compared to single junction cells. Efficiencies as high as 40% have been obtained from triple junction solar cells [1]. To obtain the maximum efficiency from a multi-junction cell, the materials of the different sub-cells have to be chosen according to the optimal band gap combination. However, in monolithic devices, it is extremely challenging to grow materials that are lattice mismatched, and this hinders one to reach the optimum sequence of band gap energies. Most current compound semiconductor solar cells are grown using lattice-matched materials. More recently, growth of lattice mismatched multi-junction solar cells has been attempted using metamorphic growth [1] and direct bonded growth techniques [2, 3]. A much larger design freedom may be achieved if nanowire heterostructures were to be implemented as in this case it is possible to combine materials with large differences in lattice constants and both radial and geometries along the growth axis can be used [4]. Therefore, nanowire tandem solar cells may enable us to achieve ultra-high efficiencies. Moreover, with a p–n junction in the radial direction, one can expect the additional advantage of decoupling light absorption and carrier collection into orthogonal directions [5]. Due to shorter carrier collection lengths, such a design would be ideal for cells of inexpensive materials with short minority carrier diffusion lengths (due to high density of impurities or defects) and hence would also be commercially favorable. Also, due to the tunable band gap energy of Silicon nanowires with diameters less than the Bohr exciton radius of its bulk form (~5 nm) [6–8], one can obtain high efficiency 2-junction solar cells by growing these nanowires with a p–n junction in the radial direction over c-Si planar p–n junction. The diameter of the nanowire, and hence the band gap energy of the upper sub-cell can be so chosen so that along with the lower sub-cell (of band gap energy 1.09 eV) the cell is able to utilize the maximum portion of the solar spectrum most efficiently.

In this work, we deduce the Detailed Balance Limit of Efficiency for the aforementioned designs. Detailed balance calculations provide the ultimate upper bound for the efficiency of a solar cell structure. Although these do not provide the exact value for the performance of a cell, they

still form a good starting point for the design. Also, the upper bound reveals how much scope for improvement one has once the structure has been fabricated.

**2 Silicon or silicon–gallium arsenide tandem cell** For sizes less than 5 nm, the band gap energy of Silicon varies with nanocrystal size. Quantum Monte Carlo calculations have predicted such a variance in band gap energy and its dependence on nanowire diameter is illustrated in Fig. 1a. [9] Here it should be noted that such a variance has also been demonstrated experimentally [10, 11]. Since the band gap energy of Si nanowires of such dimensions is greater than that of bulk Si (1.09 eV) it is possible to fabricate a 2-junction tandem cell by growing Si nanowires over crystalline silicon, c-Si. The tandem cell would consist of a dense array of radial p–n nanowire junctions over a c-Si cell. In such a design, the two sub-cells would be connected in series, i.e. the current flowing through both sub-cells is the same. We illustrate a Silicon Tandem Cell in Fig. 2.

Detailed balance calculations were performed to obtain an upper bound for the efficiency of such a design and also to find the optimum radius of nanowires at which one would obtain maximum efficiency. Light is assumed to be incident normally and a 100% packing density is

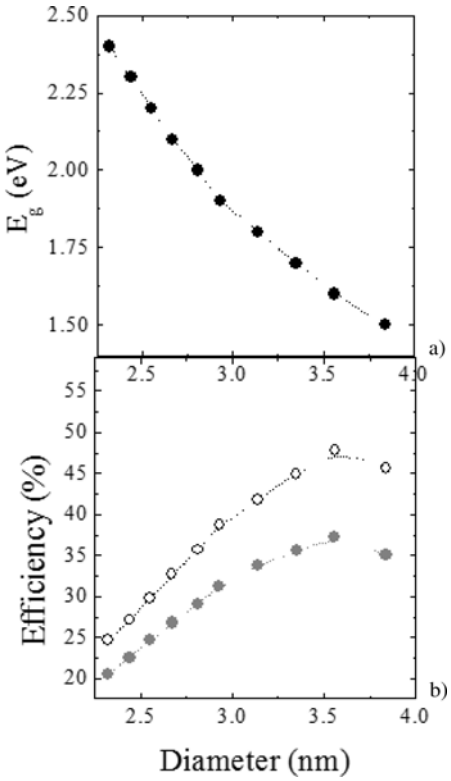


**Figure 1** a) Diameter dependence of the band gap of silicon for diameters between 2.25 nm and 4 nm. b) Efficiencies of the tandem solar cells composed of the connection in series of a c-Si and nanowire cells, as a function of the diameter of the silicon nanowire cells.

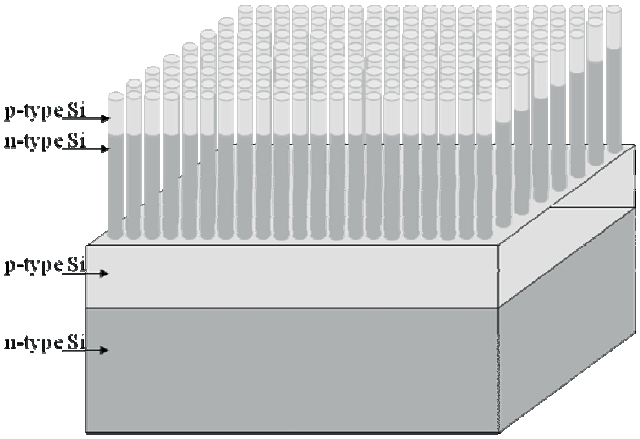


**Figure 2** Sketch of the tandem solar cell composed of the connection in series of a c-Si and nanowire cells. In this scheme, the p–n junction is realized along the growth axis of the wire.

assumed. The Sun is assumed to be a perfect blackbody at $T_s$ (6000 K) while both sub-cells are assumed to be at the same temperature $T_c$ (300 K). Also, since we are interested in obtaining an upper limit for the efficiency of the cell, we assume that every incident photon with energy greater than the band gap energy is absorbed and generates an electron hole pair.

The current, $I$, and the voltage, $V$, of the $i$-th sub-cell are related by

$$I_i = I = I_{Li} + I_{oi}\left[1 - \exp\left(\frac{qV_i}{kT_c}\right)\right]. \tag{2.1}$$

In the above expression, $q$ and $k$ refer to the electronic charge and the Boltzmann constant, and the subscripts L and o correspond to the characteristics under illumination and under dark conditions.

The black body radiation flux is given by

$$N(v,T) = \frac{2\pi}{c^2}\frac{v^2}{\exp\left(\frac{hv}{kT}\right) - 1}. \tag{2.2}$$

Expressing the light generated and the reverse saturation currents $I_{Li}$ and $I_{oi}$ in terms of the incident photon flux, $F$, at temperatures $T_s$ and $T_c$ we have

$$I_{oi} = qF_{oi}\,, \tag{2.3}$$

$$I_{Li} = q(F_{si} - F_{oi})\ [12]\,. \tag{2.4}$$

For the top sub-cell,

$$F_{o1} = 2(\pi r^2)\int_{v1}^{\infty} N(v, T_c)\,\mathrm{d}v\,,$$
$$F_{s1} = f_\omega(\pi r^2)\int_{v1}^{\infty} N(v, T_c)\,\mathrm{d}v\,, \tag{2.5}$$

 

while for the bottom sub-cell we have

$$F_{o2} = 2\left(4r^2\right)\int_{v2}^{\infty} N(v, T_c)\,\mathrm{d}v\,,$$

$$F_{s2} = f_\omega\left(\pi r^2\right)\int_{v2}^{v1} N(v, T_s)\,\mathrm{d}v + f_\omega\left[(4-\pi)\,r^2\right]\int_{v1}^{\infty} N(v, T_s)\,\mathrm{d}v\,. \tag{2.6}$$

In the above expressions $r$ is the radius if the two nanowires and $hv1$ and $hv2$ are the band gap energies of the upper and lower sub-cells respectively. Also, $f_\omega$ is a geometrical factor that takes into account the angle of incidence of the radiation and the solid angle subtended by the sun on the cell [12]. Note that the radiation incident on the portion of the lower sub-cell exactly below the first sub-cell only comprises photons with energy less than $hv1$. Therefore in this portion, only those photons with energy between $hv1$ and $hv2$ generate electron hole pairs. The remaining region of area $(4 - \pi)\,r^2$ of the lower sub-cell however receives the entire solar radiation and here all photons with energy greater than $hv2$ generate electron hole pairs. Also, while evaluating the light generated current for each sub-cell, we neglect the effect of the electroluminescence of the other sub-cell, since its final contribution to the detailed balance limit of efficiency has been shown to be negligibly small [13].

Using the above expressions the total power

$$P = \sum_{i=1}^{2} V_i I_i = \sum_{i=1}^{2} I\,\ln\left(\frac{I_{Li} + I_{oi} - I}{I_{oi}}\right). \tag{2.7}$$

The combination giving the maximum power can be obtained by solving

$$\frac{\mathrm{d}P}{\mathrm{d}I} = 0\,. \tag{2.8}$$

Also, the incident power is given by

$$P_{inc} = \left(4r^2\right) f_\omega \frac{2\pi h}{c^2}\int_0^{\infty} \frac{v^3\,\mathrm{d}v}{\exp\left(\dfrac{hv}{kT_c}\right) - 1} = \frac{2\pi\left(4r^2\right) f_\omega\,(kT_s)^4}{15h^3c^2}\,. \tag{2.9}$$

Cell efficiencies were evaluated for concentrated ($f_\omega = 1$) as well as unconcentrated sunlight ($f_\omega = 2.18 \times 10^{-5}$ for normal incidence) for a range of top-cell band gap energies, by varying the radius of the nanowires (Again, the calculation were realized assuming the 6000 K black body emission for the incident radiation). The results of the calculations are illustrated in Fig. 1b. Maximum efficiencies of 48% and 37% were obtained for concentrated and unconcentrated sunlight respectively, for top-cell band gap energy of 1.6 eV (nanowire diameter of 3.6 nm). Nanowires with diameters between 3 nm and 4 nm have already been obtained, meaning that this design is experimentally realistic.

A similarly interesting alternative is to substitute the silicon nanowire top tandem cell by a III–V nanowires with the ideal band gap. As a matter of fact, it has been demonstrated that III–V nanowires can be grown perpendicularly on Si. This means that, alternatively, one could imagine fabricating the top tandem cell with a material that has the optimal gap for the tandem combination. As shown in Fig. 2, the optimal band gap for the top cell is 1.6 eV, which could be obtained with $Al_xGa_{1-x}As$ with an Al content of $x = 0.18$. Also, fabricating the top cell with GaAs would also give good efficiencies (32% for non concentrated light). One of the main advantages of a silicon/gallium arsenide based tandem cell is that now the nanowires are not limited to homogeneous and ultra small diameters. One could imagine realizing the top cell with nanowires of 100 nm in diameter. Moreover, the diameter distribution could be relatively large, without affecting the final output of the solar cell.

Considerations on the practical implementation of the proposed structures, specially on the doped configurations, will be presented in Section 4.

**3 Nanowire tandem cell** The advantages of a nanowire tandem cell have been highlighted above. In the following, we perform detailed balance calculations for nanowire tandem cells with p–n junctions in the radial directions with the intention of tapping the additional advantage of decoupling the light absorption and carrier collection into orthogonal directions. Such a 3-junction nanowire cell is illustrated in Fig. 3. With prevailing technologies, it was not feasible to imagine a design where the individual sub-cells of the nanowire are independently connected, i.e. one where each sub-cell has a different voltage $V_i$ across its junction. This is the reason why we have only considered the sub-cells connected in parallel, i.e. they all operate at a common voltage $V$. However, Detailed Balance calculations for this design revealed efficiencies that were lower than those obtained for single junction cells.

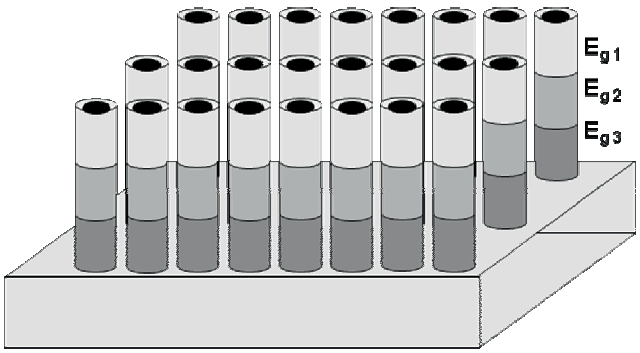


**Figure 3** Drawing of the three junction nanowire tandem solar cell. The nanowires are grown perpendicularly to the handle substrate. Within the wire, three different materials with different band gap energies are grown successively. The materials are ordered from larger to smaller energy gaps, with respect to the direction of the incident light.

These results were rather surprising since one expects a greater portion of the solar spectrum to be utilized and hence greater efficiencies. We present below a mathematical proof that explains the results obtained from the detailed balance calculations.

The light generated and the reverse saturated currents are expressed as in Eqs. (2.3) and (2.4). For the topmost sub-cell ($i = 1$) we obtain

$$F_{oi} = 2A\int_{v(i)}^{\infty} N(v,T_c)\,dv,$$
$$F_{si} = f_\omega A\int_{v(i)}^{\infty} N(v,T_s)\,dv, \tag{3.1}$$

while for the remaining sub-cells ($i \neq 1$)

$$F_{oi} = 2A\int_{v(i)}^{\infty} N(v,T_c)\,dv,$$
$$F_{si} = f_\omega A\int_{v(i)}^{v(i-1)} N(v,T_s)\,dv. \tag{3.2}$$

Here, the band gap energy of the $i$-th sub-cell is $hv(i)$.

The power obtained from the device is

$$P_{tandem} = \sum_{i=1}^{N} V_i I_i = V\sum_{i=1}^{N} I_i = qV\left[\sum_{i=1}^{N} F_{si} - \exp\left(\frac{qV}{kT_c}\right)\sum_{i=1}^{N} F_{oi}\right]. \tag{3.3}$$

Consider the first term in the summation,

$$\sum_{i=1}^{N} F_{si} = f_\omega A \times \left[\int_{v(1)}^{\infty} N(v,T_s)\,dv + \int_{v(2)}^{v(1)} N(v,T_s)\,dv + \ldots \int_{v(N)}^{v(N-1)} N(v,T_s)\,dv\right]$$
$$= f_\omega A\int_{v(N)}^{\infty} N(v,T_s)\,dv. \tag{3.4}$$

From (3.3) and (3.4) the output power can now be written as

$$P_{tandem} = qVf_\omega A\int_{v(N)}^{\infty} N(v,T_s)\,dv - qV\exp\left(\frac{qV}{kT_c}\right)\sum_{i=1}^{N} F_{oi}. \tag{3.5}$$

We shall now compare this expression with the output power of a single junction planar cell of a material of band gap energy $hv(N)$:

$$P_{single} = IV = V\left[qF_{sN} - qF_{oN}\exp\left(\frac{qV}{kT_c}\right)\right],$$
$$P_{single} = qVf_\omega A\int_{v(N)}^{\infty} N(v,T_s)\,dv - qV\exp\left(\frac{qV}{kT_c}\right)F_{oN}. \tag{3.6}$$

Comparing (3.5) and (3.6), we note that the first terms in both expressions are identical. And since

$$F_{oN} \le \sum_{i=1}^{N} F_{oi}, \tag{3.7}$$

we have

$$P_{single} \ge P_{tandem}. \tag{3.8}$$

Therefore the detailed balanced limit of efficiency for a tandem cell with the sub-cells connected in parallel would always be less than that of a single junction solar cell with the same band gap energy as the lowest sub-cell in the tandem structure.

**4 Future challenges and directions** In order to realize the silicon tandem cell proposed above, it is necessary to have a well oriented, closely spaced array of silicon nanowires with p–n junctions in the radial direction grown over a planar Silicon cell. The preferred growth of Silicon nanowires has been the Vapor–Liquid–Solid (VLS) technique [14], primarily using gold as the VLS catalyst. However, gold diffuses into the Silicon nanowires and is known to form deep level traps [15]. This greatly limits the minority carrier lifetimes and hence would inhibit the efficiency of the cell. Therefore, it is necessary to look to alternative catalysts that would not form such deep level traps. Several groups have successfully demonstrated Silicon nanowire growth for catalysts such as $TiSi_2$, Ti, Pt, Cu and Al [16–20]. For impurities such as Al, the energy levels within the band gaps are very close to the valence band edge and act therefore act as shallow acceptors rather than deep level traps.

In order to obtain a well oriented array of nanowires by VLS, one requires a periodic arrangement of catalyst droplets on the substrate. This has been achieved via different techniques such as nanosphere lithography [24], deposition of catalyst in the pores of a nanoporous alumina template [25], and even by annealing of thin metal (catalyst) films deposited on the substrate. Nanowire arrays have also been successfully fabricated by a combination of metal induced etching and nanosphere lithography [26]. However, with the aforementioned techniques, dense arrays of nanowires with diameters less than 5 nm and lengths over 1 micron are yet to be reported. One of the problems is that nanowires in the size range below 5 nm grow in the {112} direction, meaning that such a substrate would be required. However sub-5nm nanowire arrays can be achieved by thermal oxidation in dry $O_2$ of an array produced by one of the above techniques followed by etching away the oxide layer [27–29]. A second problem that could occur with long arrays of sub-5 nm silicon nanowires is that they may stick together by Van der Waals forces. From this point of view, alternative solutions like micro-porous silicon or branched nanowire structures should be considered [30, 31]. Additionally, it should be demonstrated that the

 

surface, interface and bulk defects in the nanowire structures are superior with respect to other one-dimensonal nanocrystalline silicon structures, such as the mentioned porous silicon [32].

Synthesis of nanowires with heterostructures along the wires has also been reported recently [21–23]. For growth of the p-region, p-dopant gas is introduced along with the other precursors. Subsequently if the flow of the p-dopant gas is stopped, and n-type dopant gas is introduced to the surface, under appropriate conditions, reactant activation at the catalyst site would result in n-doping of the nanowire and hence, formation of the p–n junction along the wire. Alternatively, the n- and p-dopants could also be introduced by ion implantation [33]. By implanting the species at different energies, a p–n junction can be easily obtained.

These concepts can be extended to achieve nanowires with p–n junctions in the radial direction. As an example, recently it has been demonstrated by Molecular Beam Epitaxy that it is possible to switch between one-dimensional nanowire growth to planar growth on the facets of the nanowires, with atomic precision [34]. With this technique, it is possible to deposit any kind of layer on the facets of the nanowires, as for standard MBE. As a consequence, there are no limits in the combination of materials and/or doping in the radial direction.

Nanowire tandem cells, as proposed previously, could be realized by synthesis of nanowires with heterostructures along the growth axis, followed by the deposition of an external doped layer doping in order to achieve the p–n junction in the radial direction. Metal contacts could be made to the outer shell and the inner core by Atomic Layer Deposition (ALD). However, ultra-high efficiencies can only be achieved with such a design once we are able to develop technologies to connect independently the subcells in the nanowire. Although not discussed here, nanowire tandem cells along the radial direction of the nanowire adds a new degree of freedom and should probably be considered in the future.

As a conclusion, we have calculated the use of nanowires for solar cell applications. We have shown that a silicon tandem cell can be achieved by growing sub-5 nm p–n junction in the radial direction of the Si nanowires on a planar c-Si cell. We obtained the maximum detailed balance limit of efficiency to be 48% and 37% for concentrated and unconcentrated sunlight, respectively, for a nanowire diameter of 3.6 nm. The same efficiency would be obtained if the top tandem cell would be realized with AlGaAs nanowires, with an Al content of 18%. We also demonstrate that for a parallel connection of the sub cells, the detailed balance limit of efficiency for the tandem cell will always be lower than the optimized single junction. These results are important for the future consideration of nanowires in solar cell applications.

**Acknowledgements** This research was supported by Marie Curie Excellence Grant “SENFED”, the DFG Excellence Cluster Nanosystems Initiative München (NIM) and SFB 631. The authors thank Prof. G. Abstreiter for helpful discussions.

## References

[1] R. R. King, D. C. Law, K. M. Edmondson, C. M. Fetzer, G. S. Kinsey, H. Yoon, R. A. Sherif, and N. H. Karam, Appl. Phys. Lett. **90**, 183516 (2007).
[2] A. F. I. Morral, J. M. Zahler, S. P. Ahrenkiel, M. Wanlass, and H. A. Atwater, Appl. Phys. Lett. **83**, 26 (2003).
[3] K. Tanabe, A. F. I. Morral, D. J. Aiken, M. W. Wanlass, and H. A. Atwater, Appl. Phys. Lett. **89**, 102106 (2006).
[4] F. Glas, Phys. Rev. B **74**, 121302 (2006).
[5] B. M. Kayes, N. Lewis, and H. A. Atwater, J. Appl. Phys. **97**, 114302 (2005).
[6] V. Lehmann and U. Gösele, Adv. Mater. **4**, 114 (1992).
[7] D. J. Lockwood, Solid State Commun. **92**, 101 (1994).
[8] G. D. Sanders and Yia-Chung Chang, Phys. Rev. B **45**, 9202 (1992).
[9] A. Puzder, A. J. Williamson, J. C. Grossman, and G. Galli, J. Chem. Phys. **117**, 6721 (2002).
[10] J. S. Biteen, N. S. Lewis, H. A. Atwater, and A. Polman, Appl. Phys. Lett. **84**, 5389 (2004).
[11] J. Heitmann, F. Muller, M. Zacharias, and U. Gösele, Adv. Mater. **17**, 795 (2005).
[12] W. Shockley and H. J. Quiesser, J. Appl. Phys. **32**, 510 (1961).
[13] A. D. Vos, J. Phys. D, Appl. Phys. **13**, 839 (1980).
[14] R. S. Wagner and W. C. Ellis, Appl. Phys. Lett. **4**, 89 (1964).
[15] J. R. Morante, J. E. Carceller, A. Herms, P. Cartujo, and J. Barbolla, Appl. Phys. Lett. **41**, 656 (1982).
[16] T. I. Kamins, R. Stanley Williams, Y. Chen, Y.-L. Chang, and Y. A. Chang, Appl. Phys. Lett. **76**, 562 (2000).
[17] S. Sharma, T. I. Kamins, and R. Stanley Williams, J. Cryst. Growth **267**, 613 (2004).
[18] E. C. Garnett, W. Liang, and P. Yang, Adv. Mater. **19**, 2946 (2007).
[19] J. Arbiol, B. Kalache, P. R. I. Cabarrocas, J. R. Morante, and A. F. I. Morral, Nanotechnology **18**, 305606 (2007).
[20] Y. Wang, V. Schmidt, S. Senz, and U. Gösele, Nature Nanotechnology **1**, 186 (2006).
[21] Y. Wu, R. Fan, and P. Yang, Nano Lett. **2**, 83 (2002).
[22] L. Pan, Kok-Keong Lew, J. M. Redwing, and E. C. Dickey, Microsc. Microanal. **11**, Suppl. 2 (2005).
[23] M. S. Gudikson, L. J. Lauhon, J. Wang, D. C. Smith, and C. M. Lieber, Nature **415**, 617 (2002).
[24] B. Fuhrmann, H. S. Leipner, and H.-R. Hoche, Nano Lett. **5**, 2524 (2005).
[25] T. E. Bogart, S. Dey, Kok-Keong Lew, S. E. Mohney, and J. M. Redwing, Adv. Mater. **17**, 114 (2005).
[26] K. Peng, M. Zhang, A. Lu, Ning-Bew Wong, R. Zhang, and Shuit-Tong Lee, Appl. Phys. Lett. **90**, 163123 (2007).
[27] H. I. Liu, D. K. Biegelsen, F. A. Ponce, N. M. Johnson, and R. F. W. Pease, Appl. Phys. Lett. **90**, 1383 (1994).
[28] A. R. Guichard, D. N. Barsic, S. Sharma, T. I. Kamins, and M. L. Brongersma, Nano Lett. **6**, 2140 (2006).
[29] N. Singh, A. Agarwal, L. K. Bera, T. Y. Liow, R. Yang, S. C. Rustagi, C. H. Tung, R. Kumar, G. Q. Lo, N. Balasubramanian, and D. L. Kwong., IEEE Electron Device Lett. **27**, 383 (2006).

[30] V. Lehmann and U. Gösele, Appl. Phys. Lett. **58**, 856 (1991).
[31] K. A. Dick, K. Deppert, S. Karlsson, W. Seifert, L. R. Wallenberg, and L. Samuelson, Nano Lett. **6**, 2842 (2006).
[32] H. Zimmermann, F. H. Cocks, and U. Gösele, Mater. Chem. Phys. **32**, 310 (1992).
[33] A. Colli, A. Fasoli, C. Ronning, S. Pisana, S. Piscanec, and A. C. Ferrari, Nano Lett. **8**, 1358 (2008).
[34] A. Fontcuberta i Morral, D. Spirkoska, J. Arbiol, M. Heigoldt, J. R. Morante, and G. Abstreiter, Small **4**, 899 (2008).

 